Leaf-excluded percolation in two and three dimensions

Zongzheng Zhou, Xiao Xu, Timothy M. Garoni, and Youjin Deng

Phys. Rev. E **91**, 022140 — Published 27 February 2015

DOI: 10.1103/PhysRevE.91.022140

Leaf-excluded percolation in two and three dimensions

Zongzheng Zhou,[1] Xiao Xu,[2] Timothy M. Garoni,[1,*] and Youjin Deng[2,†]

[1]*School of Mathematical Sciences, Monash University, Clayton, Victoria 3800, Australia*
[2]*Hefei National Laboratory for Physical Sciences at Microscale and Department of Modern Physics, University of Science and Technology of China, Hefei, Anhui 230026, China*

We introduce the *leaf-excluded* percolation model, which corresponds to independent bond percolation conditioned on the absence of leaves (vertices of degree one). We study the leaf-excluded model on the square and simple-cubic lattices via Monte Carlo simulation, using a worm-like algorithm. By studying wrapping probabilities, we precisely estimate the critical thresholds to be 0.355 247 5(8) (square) and 0.185 022(3) (simple-cubic). Our estimates for the thermal and magnetic exponents are consistent with those for percolation, implying that the phase transition of the leaf-excluded model belongs to the standard percolation universality class.

PACS numbers: 05.50.+q, 05.70.Jk, 64.60.ah, 64.60.F-
Keywords: Percolation, critical phenomena, universality class

I. INTRODUCTION

Graphical models, i.e. statistical-mechanical models in which the configuration space consists of certain bond configurations drawn on a lattice, play a fundamental role in the theory of critical phenomena. Examples include percolation, and more generally the Fortuin-Kasteleyn random-cluster model, as well as dimers and various loop models. In the latter two cases, the models are in fact examples of "forbidden-degree" models, in which only bond configurations which preclude specified vertex degrees are allowed; for dimers, all degrees higher than 1 are forbidden, while loop models forbid all odd degrees.

In this article, we introduce and study another example of a forbidden-degree model, the *leaf-excluded* model, which forbids bond configurations containing vertices of degree 1 (i.e. *leaves*). Consider a finite connected graph $G = (V, E)$, and let

$$\Omega = \{A \subseteq E : \ d_A(i) \neq 1\}, \tag{1}$$

where $d_A(i)$ denotes the degree of vertex i in the spanning subgraph (V, A). As an example, Fig. 1 illustrates a typical element of Ω in the case where G is a 6×6 patch of the square lattice. In this case, Ω is the set of all ways of drawing bond configurations such that each site has degree 0, 2, 3 or 4.

The leaf-excluded model on G chooses random configurations $A \in \Omega$ according to the distribution

$$\mathbb{P}(A) \propto v^{|A|}, \tag{2}$$

where $v > 0$ is a (temperature-like) bond fugacity, and $|A|$ denotes the number of bonds in the configuration A.

The model defined by (1) and (2) is equivalent to considering standard independent bond percolation and conditioning on the absence of leaves. This conditioning then introduces non-trivial correlations between the edges. Note that, on the square lattice, if we additionally forbid degree 3 vertices, the resulting model coincides with the high temperature (and low temperature) expansion of the Ising model. On the square lattice therefore, the definition of the leaf-excluded model lies precisely half way between the definitions of standard percolation (no vertex degrees forbidden) and the Ising loop representation (both leaves and degree 3 vertices forbidden). It is therefore natural to ask to which universality class does the leaf-excluded model belong?

One of the main goals of percolation theory in recent decades has been to understand the geometric structure of percolation clusters, following the pioneering work of Stanley [1]. Recently, the present authors [2] studied the geometric structure of percolation clusters by classifying the bridges present in clusters into two types: branches and junctions. A bridge was defined to be a branch if and only if at least one of the two clusters produced by its deletion is a tree. It was found that the leaf-free clusters, obtained by deleting the branches from percolation clusters, have the same fractal dimension and hull dimension as the original percolation clusters.

The set of all such leaf-free configurations coincides with Ω as defined in (1). We emphasize, however, that in [2] these configurations were generated by applying a *burning algorithm* [3] to standard bond percolation configurations, whereas in the current work they are sampled directly from the distribution (2). The probability distribution on these configurations studied in [2] is therefore very different to the distribution that we consider here. Nevertheless, based on the observations from [2], one might expect that the leaf-excluded model should belong to the percolation universality class. In this article, we present a careful numerical study which confirms this picture.

Due to the non-trivial combinatorial constraint inherent in the definition of Ω, to efficiently generate random samples from the leaf-excluded model requires a suitable Markov-chain Monte Carlo algorithm. We introduce a

*Electronic address: tim.garoni@monash.edu
†Electronic address: yjdeng@ustc.edu.cn

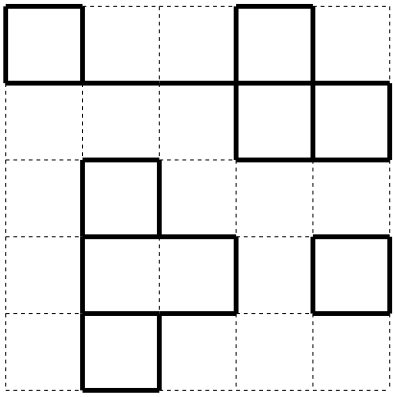

FIG. 1: A typical configuration (denoted by bold edges) of the leaf-excluded model on a 6×6 patch of the square lattice.

worm-like algorithm for this purpose. Using this algorithm, we simulate the leaf-excluded model on the square and simple-cubic lattices with periodic boundary conditions. We estimate the critical threshold v_c by studying the finite-size scaling of wrapping probabilities. Wrapping probabilities are believed to be universal, and have been successfully applied to the estimation of critical thresholds of several models [4–6]. By simulating precisely at our estimated v_c, we then estimate the thermal exponent $y_t = 1/\nu$ and magnetic exponent $y_h = d - \beta/\nu$. Here the exponent β describes the critical scaling of the percolation probability $P_\infty \sim (v - v_c)^\beta$, while ν describes that of the correlation length $\xi \sim |v - v_c|^{-\nu}$. Our results for critical exponents and universal amplitudes strongly suggest that the phase transition of the leaf-excluded model belongs to the standard percolation universality class.

The remainder of this paper is organized as follows. Sec. II introduces the worm-like algorithm and the observables measured in our simulations. Numerical results are summarized and analyzed in Section III. A brief discussion is then given in Section IV.

II. ALGORITHM AND OBSERVABLES

A. Monte Carlo algorithm

In this section we describe a Markov-chain Monte Carlo algorithm for simulating the leaf-excluded model, which is similar in spirit to a worm algorithm [7]. Worm algorithms provide very effective tools for simulating models on configuration spaces which are subject to nontrivial combinatorial constraints. The key idea underlying worm algorithms is to first enlarge the configuration space by including "defects", and to then move these defects via random walk. Numerical studies have shown that worm algorithms typically provide highly efficient Monte Carlo methods [8–12].

To simulate the leaf-excluded model, we therefore consider an enlarged configuration space in which up to two leaves are permitted. For clarity, it is convenient to define the algorithm on an arbitrary (finite and connected) graph $G = (V, E)$. The space of worm configurations is then

$$\mathcal{S} = \{(A, u, v) \in E \times V^2 : d_A(i) \neq 1 \text{ for } i \neq u, v\}.$$

The algorithm proceeds as follows. Let $\triangle$ denote symmetric difference of sets. At each time step, we perform precisely one of the following three possible updates, chosen at random with respective probabilities p_1, p_2, p_3:

1. Set $(A, u, v) \mapsto (A, v, u)$
2. Choose uniformly random $w \in V$ and set $(A, u, v) \mapsto (A, w, v)$ if $d_A(u) \neq 1$ and $d_A(w) \neq 1$.
3. Do the following:
   (a) Choose uniformly random $w \sim u$
   (b) Propose $(A, u, v) \mapsto (A \triangle uw, w, v)$, and accept with probability $\min[1, v^{|A \triangle uw| - |A|}]$, provided $(A \triangle uw, w, v) \in \mathcal{S}$.

After each update, if the new state is leaf-excluded, we measure observables. In our simulations, we used $p_1 = p_2 = 1/4$ and $p_3 = 1/2$.

We note that, unlike the case of the worm algorithm for the Ising model [7], there is no particular reason for using two defects in our algorithm, and in fact the above algorithm can be easily modified to use any fixed number of defects; including one defect. We also note that it would be somewhat of a misnomer to refer to the above algorithm as a *worm* algorithm; for a state $(A, u, v) \in \mathcal{S}$, it will not be true in general that u and v are connected by occupied bonds, and so in general there is no *worm* as such. This is in contrast to worm algorithms for Eulerian subgraphs (e.g. Ising high temperature graphs), where the handshaking lemma demands that the two defects be connected.

B. Sampled quantities

We simulated the leaf-excluded model on the $L \times L$ square lattice for system sizes up to $L = 1024$, and on the $L \times L \times L$ simple-cubic lattice for system sizes up to $L = 96$. For each system size, approximately 10^8 samples were produced.

For each sampled leaf-excluded bond configuration, we measured the following observables.

1. The number of occupied bonds $\mathcal{N}_b$.
2. The size of the largest cluster $\mathcal{C}_1$.
3. The cluster-size moments $\mathcal{S}_m = \sum_{\mathcal{C}} |\mathcal{C}|^m$ with $m = 2, 4$, where the sum is over all clusters $\mathcal{C}$.

4. The indicators $\mathcal{R}^{(x)}$, $\mathcal{R}^{(y)}$, $\mathcal{R}^{(z)}$ for the event that a cluster wraps around the lattice in the x, y, or z direction, respectively.

From these observables, we calculated the following quantities:

1. The mean size of the largest cluster $C_1 = \langle \mathcal{C}_1 \rangle$, which scales as $\sim L^{y_h}$ at the critical point v_c.

2. The mean size of the cluster at the origin, $\chi = \langle \mathcal{S}_2 \rangle / L^d$, which at v_c scales as $\sim L^{2y_h - d}$.

3. The dimensionless ratios

$$Q_1 = \frac{\langle {\mathcal{C}_1}^2 \rangle}{\langle \mathcal{C}_1 \rangle^2} , \quad Q_2 = \frac{\langle 3{\mathcal{S}_2}^2 - 2\mathcal{S}_4 \rangle}{\langle {\mathcal{S}_2}^2 \rangle} . \tag{3}$$

4. The probability that a winding exists in the x direction $R^{(x)} = \langle \mathcal{R}^{(x)} \rangle$. In two dimensions, we also measured $R^{(2)} = \langle \mathcal{R}^{(x)} \mathcal{R}^{(y)} \rangle$, and in three dimensions measured $R^{(3)} = \langle \mathcal{R}^{(x)} \mathcal{R}^{(y)} \mathcal{R}^{(z)} \rangle$. $R^{(d)}$ gives the probability that windings simultaneously exist in all d possible directions.

5. The covariance of $\mathcal{R}^{(x)}$ and $\mathcal{N}_b$

$$g_{bR}^{(x)} = \langle \mathcal{R}^{(x)} \mathcal{N}_b \rangle - \langle \mathcal{R}^{(x)} \rangle \langle \mathcal{N}_b \rangle, \tag{4}$$

which is expected to scale as $\sim L^{y_t}$ at the critical point.

III. RESULTS

A. Fitting methodology

We began by estimating the critical point v_c by performing a finite-size scaling analysis of the ratios Q_1, Q_2 and wrapping probabilities $R^{(x)}$, $R^{(d)}$. The MC data for these quantities were fitted to the ansatz

$$\mathcal{O}(\epsilon, L) = \mathcal{O}_c + \sum_{k=1}^{2} q_k \epsilon^k L^{k y_t} + b_1 L^{y_i} + b_2 L^{y_2} , \tag{5}$$

where $\epsilon = v_c - v$, y_i and y_2 are respectively the leading and sub-leading correction exponents, and $\mathcal{O}_c = \mathcal{O}(\epsilon = 0, L \to +\infty)$ is a universal constant. The parameters q_k, b_1, b_2 are non-universal amplitudes.

We then performed extensive simulations at our best estimate of v_c, in order to estimate the critical exponents y_t and y_h. These exponents were obtained by fitting $g_{bR}^{(x)}$, C_1 and χ to the ansatz

$$\mathcal{O}(L) = L^{y_\mathcal{O}} (a_0 + b_1 L^{y_i} + b_2 L^{y_2}) , \tag{6}$$

where $y_\mathcal{O}$ equals y_t for $g_{bR}^{(x)}$, y_h for C_1 and $2y_h - d$ for χ, and a_0 is a non-universal constant. In all fits reported below, we fixed $y_2 = -2$, which corresponds to the exact value of the sub-leading correction exponent [13] for percolation.

As a precaution against correction-to-scaling terms that we failed to include in the fit ansatz, we imposed a lower cutoff $L \geq L_{\min}$ on the data points admitted in the fit, and we systematically studied the effect on the χ^2 value of increasing $L_{\min}$. Generally, the preferred fit for any given ansatz corresponds to the smallest $L_{\min}$ for which the goodness of fit is reasonable and for which subsequent increases in $L_{\min}$ do not cause the χ^2 value to drop by vastly more than one unit per degree of freedom. In practice, by "reasonable" we mean that $\chi^2/\mathrm{DF} \lessapprox 1$, where DF is the number of degrees of freedom.

We analyze the data on the square lattice in Sec. III B and Sec. III C. The results on the simple cubic lattice are shown in Sec. III D.

B. Square lattice near v_c

We first study the critical behavior of $R^{(x)}$, $R^{(d)}$ and Q_1, Q_2 near v_c. Fig. 2 plots $R^{(x)}$ and Q_1 versus v. Clearly, $R^{(x)}$ suffers from only very weak corrections to scaling.

We begin by considering $R^{(x)}$. Setting $b_2 = 0$ and leaving y_i free, we were unable to obtain a stable estimate of y_i. The fits with two correction terms included (fixing $y_i = -1$) show that b_1 is consistent with zero and $b_2 = 2(1)$ for $L_{\min} = 64$. In fact, the data for $R^{(x)}$ with $L_{\min} = 128$ can be well fitted even with fixed $b_1 = b_2 = 0$. We also perform fits with only one of $b_1 L^{-1}$ or $b_2 L^{-2}$ included. Comparing the various fit results, we estimate $v_c = 0.355\,247\,5(5)$ and $y_t = 0.752(3)$. The latter is clearly consistent with 3/4 for two-dimensional percolation. We also estimate the universal amplitude $R_c^{(x)} = 0.521\,2(2)$, consistent with the exact value $0.521\,058\,290$ [14, 15].

The fits of $R^{(d)}$ show that it suffers even weaker finite-size corrections. The amplitudes b_1 and b_2 are both consistent with zero for $L_{\min} = 16$. Again, we also perform fits in which we include only one of these corrections, and also fits in which we include neither. We then estimate $v_c = 0.355\,247\,4(5)$, $y_t = 0.754(3)$ and $R_c^{(d)} = 0.351\,7(1)$, the latter of which is consistent with the exact value $0.351\,642\,855$ for standard percolation [14, 15].

Finally, we fit the data for Q_1 and Q_2. The fits predict a leading correction exponent $y_i = -1.57(5)$ and $-1.7(1)$ respectively. We note that this is consistent with the exact value $-3/2$ [16] for two-dimensional percolation. We estimate $v_c = 0.355\,247\,5(5)$ from Q_1 and $v_c = 0.355\,247\,5(8)$ from Q_2. Both of their fits produce $y_t = 0.751(3)$. We also estimate the universal amplitudes $Q_{1,c} = 1.041\,47(5)$ and $Q_{2,c} = 1.148\,6(2)$, both of which are consistent with the estimates for standard percolation [17].

Our estimates for v_c, y_t and the universal wrapping probabilities are summarized in Tab. I, where we also report the known results for standard percolation. The results strongly suggest that the phase transition of the leaf-excluded model belongs to the standard percolation

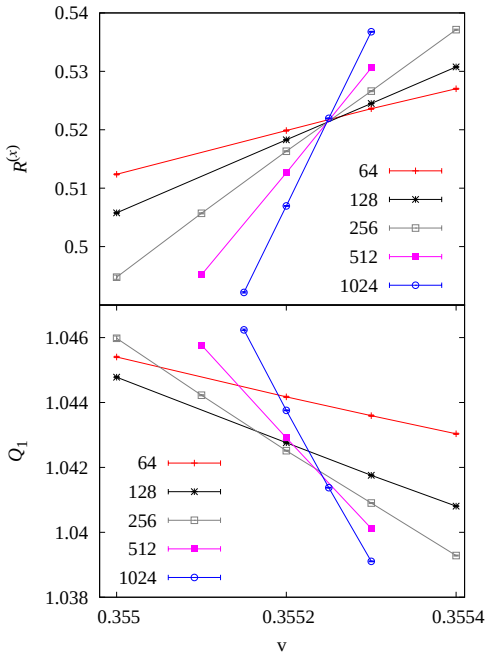

FIG. 2: Plots of $R^{(x)}$ and Q_1 versus v for the leaf-excluded model on the square lattice.

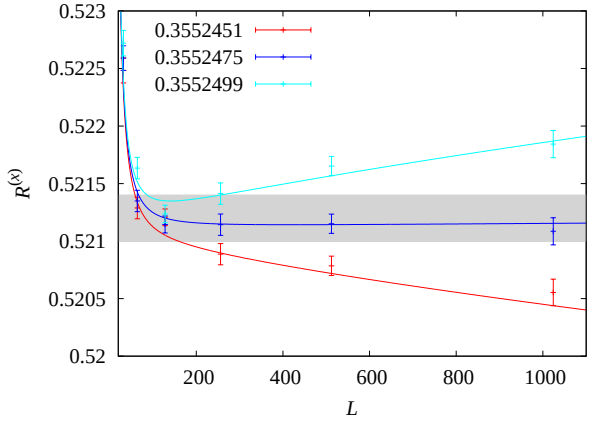

FIG. 3: Plots of $R^{(x)}(v, L)$ versus L for fixed values of v, for the two-dimensional leaf-excluded model. The curves correspond to our preferred fit of the Monte Carlo data. The shaded grey strips indicate an interval of one error bar above and below the estimate $R_c^{(x)} = 0.5212(2)$.

universality class.

In Fig. 3, we illustrate the accuracy of our estimate of v_c by plotting $R^{(x)}$ versus L with v set to our central estimate of v_c, $v = 0.355\,247\,5$, and also with v chosen three error bars above and below this estimate. Precisely at $v = v_c$, as $L \to \infty$ the data should tend to a horizontal line, whereas the data with $v \neq v_c$ should bend upward or downward. Fig. 3 provides confirmation that the true value of v_c does indeed lie in the interval

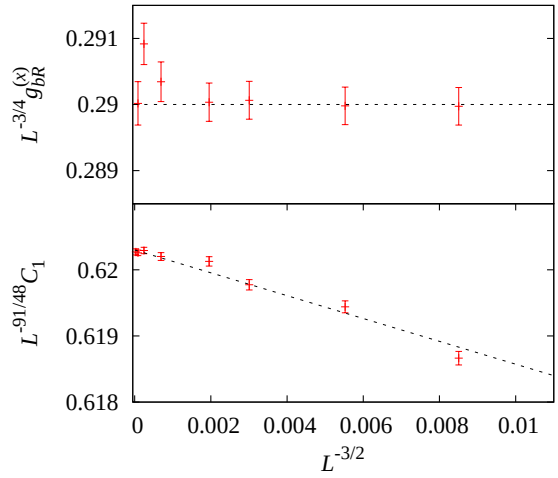

FIG. 4: Plots of $L^{-3/4} g_{bR}^{(x)}$ and $L^{-91/48} C_1$ versus $L^{-3/2}$. The straight lines are simply to guide the eye.

$(0.3552451, 0.3552499)$. Moreover, the asymptotic flatness of the $R^{(x)}$ curve at our reported central estimate of v_c strongly suggests that our estimate lies very close indeed to the true value of v_c.

C. Square lattice at v_c

To obtain final estimates of y_t and y_h, we performed high-precision simulations at a single value of v corresponding to our estimated threshold $v_c = 0.355\,247\,5$, and fitted the data for $g_{bR}^{(x)}$, C_1 and χ to (6). The leading correction exponent was set to $y_i = -3/2$.

The fits of $g_{bR}^{(x)}$ show that both the amplitudes b_1 and b_2 are consistent with zero. The data for $g_{bR}^{(x)}$ can be well fitted ($\chi^2/DF < 1$ for $L_{\min} = 24$) even without any corrections. From the fits, we estimate $y_t = 0.750(1)$, which is consistent with the estimate in Sec. III B but with improved precision.

The fits of C_1 and χ show a non-zero b_1 if only the leading correction term is included in the fits. For comparison, we also performed fits including only the $b_2 L^{-2}$ term, and including both corrections. Both of these fits suggest $y_h = 1.895\,8(1)$, which is fully consistent with the exact result $y_h = 91/48$ for two-dimensional percolation. As further illustration, Fig. 4 shows a plot of $L^{-3/4} g_{bR}^{(x)}$ and $L^{-91/48} C_1$ versus $L^{-3/2}$.

D. Simple-cubic lattice

We performed an analogous study of the leaf-excluded model on the simple-cubic lattice.

We again began by fitting the data for $R^{(x)}$, $R^{(d)}$ and Q_1, Q_2 to the ansatz (5) in order to estimate v_c. Fig. 5

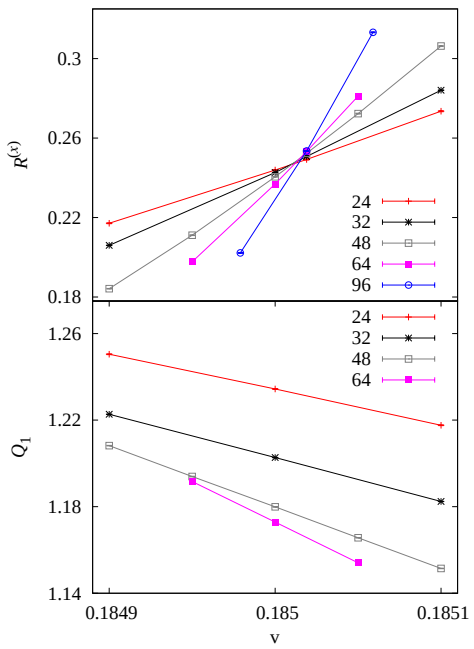

FIG. 5: Plots of $R^{(x)}$ and Q_1 versus v for the leaf-excluded model on the simple-cubic lattice.

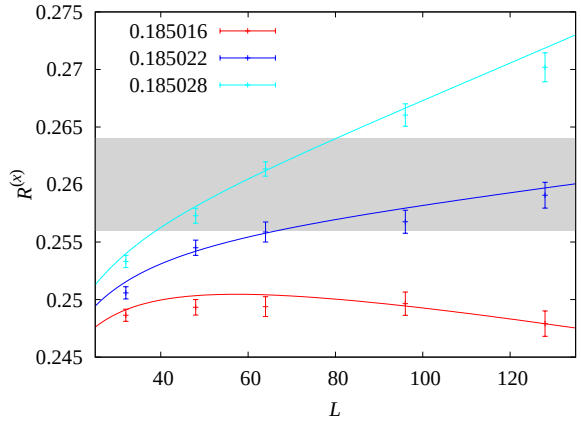

FIG. 6: Plots of $R^{(x)}(p, L)$ versus L for fixed values of p, for the three-dimensional leaf-excluded model. The curves correspond to our preferred fit of the Monte Carlo data. The shaded grey strips indicate an interval of one error bar above and below the estimate $R_c^{(x)} = 0.260(4)$.

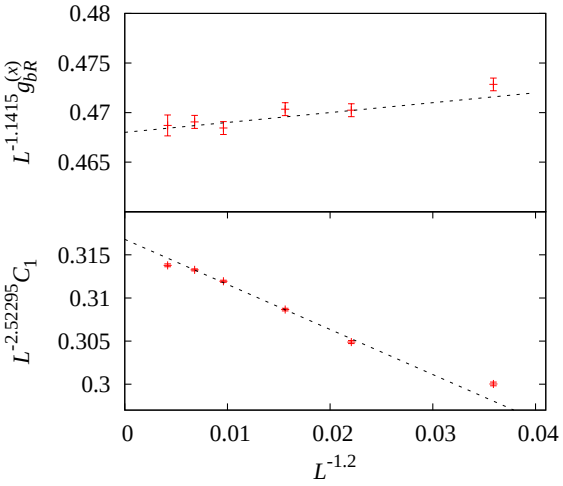

FIG. 7: Plot of $L^{-1.141\,5}g_{bR}^{(x)}$ and $L^{-2.522\,95}C_1$ versus $L^{-1.2}$. The values of the critical exponents used on the vertical axis correspond to the estimates $y_t = 1.1415(15)$ and $y_h = 2.522\,95(10)$ [4, 18]. The straight lines are simply to guide the eye.

plots $R^{(x)}$ and Q_1 versus v, which again clearly shows that $R^{(x)}$ suffers from only very weak corrections to scaling. In each case of fits, leaving y_i free resulted in unstable fits. Instead, we fixed $y_i = -1.2$, which is numerically estimated in [4] to be the leading correction exponent for three-dimensional percolation. For comparison, we performed fits with different combinations of the terms $b_1 L^{-1.2}$ or $b_2 L^{-2}$ present. The best estimates were obtained from $R^{(x)}$, which yield $v_c = 0.185\,022(3)$ and $y_t = 1.143(8)$. We also estimated the universal amplitudes $R_c^{(x)} = 0.260(4)$ and $R_c^{(d)} = 0.083(4)$. The universal amplitudes for Q_1 and Q_2 cannot be precisely estimated due to the strong finite-size corrections.

Simulating at our estimated v_c, we then fitted the data for $g_{bR}^{(x)}$, C_1, χ to the ansatz (6) to estimate y_t and y_h. Both the two correction terms were included in the fits. The fits of $g_{bR}^{(x)}$ yields $y_t = 1.142(7)$. From C_1 we estimate $y_h = 2.513(5)$. However, we find that it is difficult to estimate y_h from χ due to the strong finite-size corrections.

We again illustrate our estimated v_c by plotting $R^{(x)}$ versus L for fixed values of v around our central estimate of v_c. The figure confirms that the true value of v_c lies within two error bars of our central estimate. In this case however, the curvature suggests the central estimate lies slightly above the true value of v_c. See Fig. 6. Our estimates for the critical threshold, critical exponents and wrapping probabilities on the simple-cubic lattice are summarized in Tab. I. The agreement with the corresponding values for standard three-dimensional percolation [4] strongly suggests the leaf-excluded model is in the percolation universality class. As further illustration, Fig. 7 shows plots of $L^{-y_t} g_{bR}^{(x)}$ and $L^{-y_h} C_1$ versus L^{y_i}, using percolation exponent values taken from [4].

IV. DISCUSSION

We have introduced in this paper the leaf-excluded model, and investigated its critical behavior. Monte Carlo simulations of the leaf-excluded model were car-

d	Model	v_c	y_t	y_h	$R_c^{(x)}$	$R_c^{(d)}$	$Q_{1,c}$	$Q_{2,c}$
2	Leaf-excluded	0.355 247 5(8)	0.751(1)	1.895 8(1)	0.5212(2)	0.351 7(1)	1.041 46(10)	1.148 7(2)
	Percolation [13–15, 17]	1	3/4	91/48	0.521 058 290	0.351 642 855	1.041 48(1)	1.148 69(3)
3	Leaf-excluded	0.185 022(3)	1.143(8)	2.513(5)	0.260(4)	0.083(4)	-	-
	Percolation [4, 18]	0.331 224 4(1)	1.141 5(15)	2.522 95(15)	0.257 80(6)	0.080 44(8)	1.155 5(3)	1.578 5(5)

TABLE I: Summary of our estimates for the thresholds v_c, critical exponents y_t and y_h, and wrapping probabilities for the leaf-excluded model. A comparison with standard bond percolation is also included.

ried out on the square and simple-cubic lattices with periodic boundary conditions. By studying wrapping probabilities, we estimated the critical thresholds $v_c = 0.355\,247\,5(8)$ (square) and $v_c = 0.185\,022(3)$ (simple-cubic). The critical exponents y_t and y_h and wrapping probabilities were found to be consistent with those for standard percolation, which indicates that the phase transition of the leaf-excluded model belongs to the percolation universality class.

As mentioned in the Introduction, rather than enforcing the absence of degree 1 vertices, as we have considered in the current work, one could more generally forbid any specified set of vertex degrees. A very familiar example is to exclude odd vertices, in which case one obtains the high-temperature expansion of the Ising model. Dimer, monomer-dimer, and fully-packed loop models also fit into this framework. A general forbidden-degree model of this kind was studied on the complete graph (i.e. in mean field) from a probabilistic perspective in [19], however questions of universality were not considered. It would be of interest to understand systematically how the choice of forbidden vertex degrees affects the resulting universality class.

Finally, it would be natural to consider a generalization of (2) which included a cluster fugacity, in addition to the bond fugacity. Such a model would correspond to the Fortuin-Kasteleyn model conditioned on the absence of leaves.

V. ACKNOWLEDGMENTS

This work is supported by the National Nature Science Foundation of China under Grant No. 11275185, and the Chinese Academy of Sciences. It was also supported under the Australian Research Council's Discovery Projects funding scheme (project number DP110101141), and T.M.G. is the recipient of an Australian Research Council Future Fellowship (project number FT100100494). The simulations were carried out in part on NYU's ITS cluster, which is partly supported by NSF Grant No. PHY-0424082. In addition, this research was undertaken with the assistance of resources provided at the NCI National Facility through the National Computational Merit Allocation Scheme supported by the Australian Government. Y.J.D also acknowledges the Specialized Research Fund for the Doctoral Program of Higher Education under Grant No. 20113402110040 and the Fundamental Research Funds for the Central Universities under Grant No. 2340000034. T.M.G. is grateful for the hospitality shown by the University of Science and Technology of China at which this work was completed, particularly the Hefei National Laboratory for Physical Sciences at Microscale.

[1] H. E. Stanley, J. Phys. A **10**, L211 (1977).
[2] X. Xu, J. Wang, Z. Zhou, T. M. Garoni, and Y. Deng, Physical Review E **89**, 012120 (2014).
[3] H. J. Herrmann, D. C. Hong, and H. E. Stanley, J. Phys. A **17**, L261 (1984).
[4] J. Wang, Z. Zhou, W. Zhang, T. M. Garoni, and Y. Deng, Phys. Rev. E **87**, 052107 (2013).
[5] M. E. J. Newman and R. M. Ziff, Phys. Rev. Lett. **85**, 4104 (2000).
[6] X. Xu, J. Wang, J.-P. Lv, and Y. Deng, Frontiers of Physics **9**, 113 (2014).
[7] N. Prokof'ev and B. Svistunov, Phys. Rev. Lett. **87**, 160601 (2001).
[8] Y. Deng, T. M. Garoni, and A. D. Sokal, Physical Review Letters **99**, 110601 (2007).
[9] U. Wolff, Nuclear Physics B **810**, 491 (2009).
[10] U. Wolff, Nuclear Physics B **814**, 549 (2009).
[11] U. Wolff, Nuclear Physics B **824**, 254 (2010).
[12] U. Wolff, Nuclear Physics B **832**, 520 (2010).
[13] B. Nienhuis, J. Stat. Phys. **34**, 731 (1984).
[14] H. T. Pinson, J. Stat. Phys. **75**, 1167 (1994).
[15] R. M. Ziff, C. D. Lorenz, and P. Kleban, Physica A: Statistical Mechanics and its Applications **266**, 17 (1999).
[16] R. M. Ziff, Phys. Rev. E **83**, 020107 (2011).
[17] H. Hu, H. W. J. Blöte, and Y. Deng, Journal of Physics A: Mathematical and Theoretical **45**, 494006 (2012).
[18] J. Wang, Z. Zhou, W. Zhang, T. M. Garoni, and Y. Deng, Phys. Rev. E **89**, 069907 (2014).
[19] G. Grimmett and S. Janson, Random Structures and Algorithms **37**, 137 (2010).